

# Ultrafast Spectroscopic Study on Caffeine Mediated Dissociation of Mutagenic Ethidium from Synthetic DNA and Various Cell Nuclei

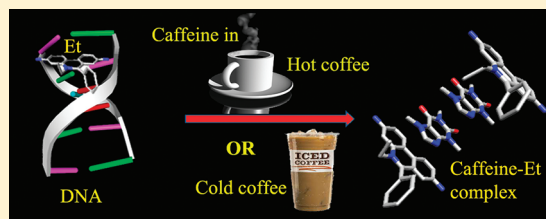
Soma Banerjee,<sup>†</sup> Debajit Bhowmik,<sup>‡</sup> Pramod Kumar Verma,<sup>†</sup> Rajib Kumar Mitra,<sup>†</sup> Anirban Sidhhanta,<sup>‡</sup> Gautam Basu,<sup>§</sup> and Samir Kumar Pal<sup>1\*,†</sup>

<sup>†</sup>Unit for Nano Science and Technology, Department of Chemical, Biological and Macromolecular Sciences, S. N. Bose National Centre for Basic Sciences, Block JD, Sector III, Salt Lake, Kolkata 700 098, India

<sup>‡</sup>Department of Biochemistry, University of Calcutta, 35 Ballygunge Circular Road, Kolkata 700 019, West Bengal, India

<sup>§</sup>Department of Biophysics, Bose Institute P 1/12, C. I. T. Road, Scheme VIIM, Kolkata 700054 West Bengal, India

**ABSTRACT:** We report a systematic investigation of caffeine-induced dissociation of ethidium (Et) cation, a potential mutagen. Time-resolved fluorescence studies are consistent with a mechanism where caffeine–Et complex formation in bulk solution drives the dissociation of DNA-bound Et. Temperature-dependent picosecond-resolved studies show the caffeine–Et complex to be stable over a wide range of temperature, within and beyond the normal physiological limit. A combination of NMR spectroscopy and dynamic light scattering experiments allowed us to propose a molecular model of the caffeine–Et complex. Caffeine-induced extraction of Et from whole cells was also performed on squamous epithelial cells collected from the inner lining of the human mouth, A549 (lung carcinoma), A375 (human skin), RAW (macrophage), and Vero (African green monkey kidney epithelium) cell lines. Interestingly the efficiency of caffeine in extracting Et has been found to be dependent on cell types. Our results both in vitro as well as ex vivo provide important clues about the efficiency and mechanism of caffeine as a potential antimutagenic therapeutic agent.



## INTRODUCTION

Molecular recognition of DNA in in vitro condition by small ligands/drugs in the presence of caffeine, a widely consumed stimulant, is well-studied.<sup>1–3</sup> Earlier, a set of studies has indicated that caffeine can diminish the cytotoxic/cytostatic effects of doxorubicin, ethidium (Et) bromide,<sup>4,5</sup> and reverses cytotoxic effect of the antitumor agent mitoxantrone, eilipticine, and doxorubicin analogues.<sup>6</sup> Spectroscopic studies on the deintercalation of Et, a potential mutagen<sup>7</sup> from genomic DNA in solution at room temperature, is also reported in the literature.<sup>8</sup> Such studies essentially intended to conclude the therapeutic use of caffeine, a xanthine alkaloid, in animal models. However, a detailed molecular picture of the deintercalation mechanism and the universal application of such xanthine alkaloids in the extraction of Et from the nucleus of various cell lines are missing from the reported studies and are among the motives of our present report. The mechanism of deintercalation both within and beyond the temperatures of physiological interest is also sparse in the reported literature and is one of the motives of the present study.

In this study we have used steady-state and picosecond-resolved fluorescence spectroscopy and time-gated fluorescence microscopy to investigate the detachment of mutagenic Et from synthesized DNA of specific sequences in vitro and various types of cell lines including squamous epithelial cells collected from the inner lining of the human mouth, A549 (lung carcinoma), A375 (human skin), RAW (macrophage), and Vero (African green monkey kidney epithelium) cells in ex vivo conditions. For the investigation of the efficacy of the caffeine-induced detachment of the intercalative mutagen from the DNA within and beyond

the physiological temperature, we have performed temperature-dependent spectroscopic measurement on the Et–DNA systems in the presence and absence of the caffeine molecule. A detailed structural analysis employing NMR experiments followed by dynamic light scattering (DLS) studies on the caffeine–Et complex explores the molecular picture of such complexes. Our time-gated fluorescence microscopic studies on various live and fixed cell lines indicate that the efficiency of Et extraction by the xanthine alkaloid is inconsistent and not very much intuitive from the above-mentioned in vitro studies.

## MATERIALS AND METHODS

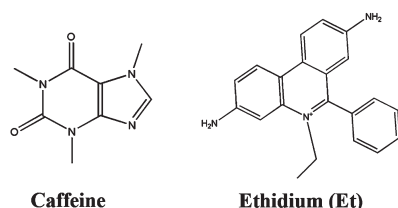
The fluorescent dyes ethidium bromide (EtBr) and DAPI were obtained from Molecular Probes while caffeine and merocyanine 540 from Fluka and used without further purification. The structures of caffeine and Et are shown in Scheme 1. While DAPI is reported to be an excellent fluorescent stain for the visualization of cell nuclei,<sup>9</sup> merocyanine 540 is found to have efficacy in fluorescent staining of unperturbed cellular membrane of viable cells.<sup>10</sup> The purified (reverse-phase cartridge) synthetic DNA oligonucleotides of 12 bases (dodecamer) with sequence CGCGAATTCGCG were obtained from TriLink. To reassociate the single-strand DNA into self-complementary ds-DNA [(CGCGAATTCGCG)<sub>2</sub>], thermal annealing was performed per the methodology prescribed by the vendor. In the present study,

**Received:** July 4, 2011

**Revised:** October 25, 2011

**Published:** October 27, 2011

## Scheme 1. Structures of Caffeine and Ethidium



the concentration of a base pair of a DNA is considered to be the overall concentration of the DNA. The nucleotide concentrations were determined by absorption spectroscopy using the average extinction coefficient per nucleotide of the DNA ( $6600 \text{ M}^{-1} \text{ cm}^{-1}$  at 260 nm). Solutions for steady-state and time-resolved studies were prepared in phosphate buffer (pH 7) while those used for cell study were prepared in phosphate buffer saline (PBS, pH 7.4) using double distilled water, except for NMR studies where the samples were prepared in HPLC water. Squamous epithelial cells were collected from human mouth, spreaded on glass slides, and stained with Et solution followed by thorough destaining under PBS. A549, A375, RAW, and Vero cells were grown in Ham's F-10 medium, 10% bovine fetal serum, 2 mM glutamine, 25 U/mL penicillin, and 25 U/mL streptomycin at 37 °C with 5%  $\text{CO}_2$ , as described previously.<sup>11</sup>

Fluorescence micrographs of squamous epithelial cells were taken using an Olympus BX51 fluorescence microscope while those of other cell lines were taken using a Nikon eclipse Ti-U inverted fluorescence microscope. The micrographs were analyzed with analySIS Five image analysis software. Steady-state absorption and emission were measured with a Shimadzu Model UV-2450 spectrophotometer and a Jobin Yvon Model Fluoromax-3 fluorimeter, respectively. All picosecond transients were measured by using commercially available (Edinburgh Instruments, Livingston, U.K.) picosecond-resolved time-correlated single-photon counting (TCSPC) setup (instrument response function (IRF) of 80 ps) using a 409 nm excitation laser source with temperature control setup from Julabo (Model F32). Fluorescence from the sample was detected by a photomultiplier after dispersing through a double grating monochromator. For all transients the polarizer in the emission side was adjusted to be at 54.7° (magic angle) with respect to the polarization axis of the excitation beam. For fluorescence anisotropy measurements, emission polarization was adjusted to be parallel or perpendicular to that of the excitation, and the anisotropy is defined as

$$r(t) = [I_{\text{para}} - GI_{\text{perp}}]/[I_{\text{para}} + 2GI_{\text{perp}}] \quad (1)$$

The magnitude of  $G$ , the grating factor of the emission monochromator of the TCSPC system, was found by long-time tail matching technique.<sup>12</sup> The temporal decay,  $r(t)$ , has been fitted with a single-exponential function,  $r(t) = r_0 \exp(-t/\tau_r)$ , where  $r_0$  is the anisotropy at time  $t = 0$ . The rotational relaxation time,  $\tau_r$ , of the fluorescent probe is related to the local microviscosity,  $\eta_m$ , experienced by the probe molecule through the Stokes–Einstein–Debye equation (SED),<sup>13,14</sup>

$$\tau_r = \eta_m V_h / k_B T \quad (2)$$

where  $k_B$  is the Boltzmann constant,  $T$  is the temperature, and  $V_H$  is the hydrodynamic volume of the probe. With use of the  $\tau_r$  value in eq 2, the hydrodynamic volume of the probe is found.

DLS measurements were done with a Nano S Malvern instrument employing a 4 mW He–Ne laser ( $\lambda = 632.8 \text{ nm}$ ) equipped with a

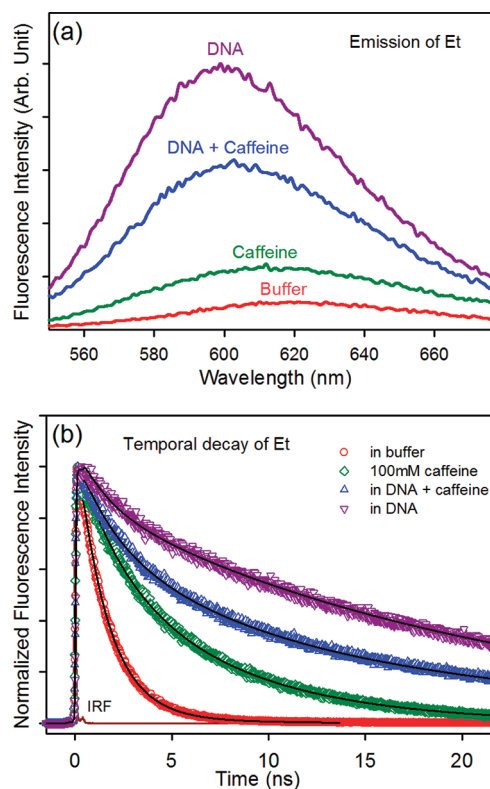


**Figure 1.** (a) Steady-state emission of ethidium in various environments. (b) Time-resolved fluorescence transients of ethidium (from bottom) in buffer, caffeine ([caffeine] = 100 mM), and DNA ([DNA]:[Et] = 8:1) in the presence and absence of caffeine.

thermostatted sample chamber. All measurements are taken at 173° scattering angle. The scattering intensity data are processed using the instrumental software to obtain the hydrodynamic diameter ( $d_H$ ) and the size distribution of the scatterer in each sample. The instrument measures the time-dependent fluctuation in intensity of the light scattered from the particles in solution at a fixed scattering angle.  $d_H$  of the particles are estimated from the intensity autocorrelation function of the time-dependent fluctuation in intensity.  $d_H$  is defined as

$$d_H = \frac{k_B T}{3\pi\eta D} \quad (3)$$

where  $k_B$  = Boltzmann constant,  $T$  = absolute temperature,  $\eta$  = viscosity, and  $D$  = translational diffusion coefficient. In a typical size distribution graph from the DLS measurement, the X-axis shows a distribution of size classes in nanometers, while the Y-axis shows the relative intensity of the scattered light.

<sup>1</sup>H NMR experiments were performed on caffeine, Et, and a mixture of the two (titrations) samples in aqueous phosphate buffer at pH 7.2 (Watergate solvent suppression) using a Bruker DRX 500 MHz spectrometer. <sup>1</sup>H signals were assigned either by comparing with literature<sup>15</sup> or by performing TOCSY and NOESY/ROESY experiments using standard protocols.

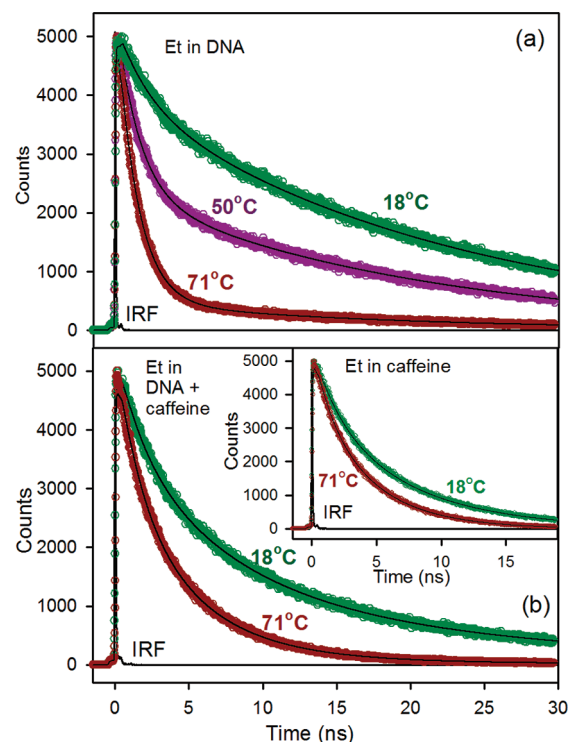
## RESULTS AND DISCUSSION

In Figure 1a,b steady-state and time-resolved studies on the Et intercalated to the synthetic DNA are presented. As shown in Figure 1a Et in water produces an emission peak at 623 nm (excited at 409 nm).<sup>16</sup> In the presence of 100 mM caffeine, the

**Table 1. Lifetime Components ( $\tau_1$ ,  $\tau_2$ ,  $\tau_3$ ) with Corresponding Amplitudes ( $A_1$ ,  $A_2$ ,  $A_3$ ) of Ethidium in Various Environments (Error,  $\pm 5\%$ )**

sample	$\tau_1$ (ns)	$A_1$ (%)	$\tau_2$ (ns)	$A_2$ (%)	$\tau_3$ (ns)	$A_3$ (%)
Et in buffer	1.6	100				
Et in 100 mM caffeine	7.0	84.5	2.3	15.5		
[Et]:[DNA] = 1:8	1.5	2	21	98		
[Et]:[DNA] = 1:8 in the presence of 100 mM caffeine	7.0	22	23	74	1.8	4

peak exhibits a blue shift to 615 nm with a subsequent increase in the intensity. The blue shift of the emission peak signifies a hydrophobic environment experienced by Et which might be due to the caffeine–Et heteroassociation as evidenced by some previous works.<sup>16,17</sup> When completely intercalated in the DNA oligomer at [DNA]:[Et] = 8:1,<sup>16</sup> the emission of Et exhibits substantial blue shift to produce the fluorescence maximum at 600 nm with an order of magnitude increase in the intensity with respect to that in water. The observed blue shift and enhanced intensity is due to strong intercalation of Et into the hydrophobic interior of the DNA.<sup>16</sup> As 100 mM caffeine solution is added into the DNA–Et complex, the emission intensity decreases with a little red shift to 605 nm. The red shift can be explained in terms of the deintercalative property of caffeine that releases a certain amount of Et from the DNA bound state either to the caffeine bound state or to the free form in the buffer. Our steady-state fluorescence emission results strongly corroborate with earlier studies.<sup>8</sup> However, conclusive spectroscopic evidence of the deintercalated Et in the heteroassociation with caffeine was absent in the earlier studies.<sup>8</sup> Deconvolution of the emission spectra of Et in DNA in the presence and absence of caffeine suggests  $\sim 40\%$  of the bound Et releases from DNA upon addition of caffeine, but whether the released Et gets bound to caffeine or remains free in the solution cannot be concluded from the steady-state results within such a narrow shift of emission maxima. A similar picture evolves from the time-resolved study (Figure 1b, Table 1). Et in buffer shows single-exponential fluorescence decay with a time constant of 1.6 ns which is close to the earlier reported values.<sup>8,16</sup> In caffeine solution the decay pattern becomes biexponential with time constants of 2.3 (15.5%) and 7.0 ns (84.5%). When intercalated in DNA, the decay pattern of Et emission gets considerably slower with time constants of 1.5 (2%) and 21 ns (98%). Note that the insignificant contribution of the fast component in the transient confirms the presence of a very low fraction of Et free in buffer. On the other hand the longer time component (21 ns) is assigned to the lifetime of Et molecules intercalated to DNA.<sup>16</sup> When 100 mM caffeine is added to Et–DNA complex the decay process becomes faster and can only be fitted triexponentially with time constants of 1.8 (4%), 7.0 (22%), and 23 ns (74%). These time constants can easily be identified with those of Et in buffer, heteroassociation with caffeine, and intercalation with DNA, respectively, and fits to the heterogeneous model of Et in the aqueous solution of DNA in the presence of caffeine. The triexponential nature of the decay pattern signifies the presence of at least three different environments of residence of Et in the solution. If the contribution from each environment is assumed to add up linearly in the total decay process, then it can be

**Figure 2.** Temperature-dependent time-resolved fluorescence transients of [DNA]:[Et] = 8:1 (a) in the absence and (b) in presence of caffeine ([caffeine] = 100 mM) and 12.5  $\mu\text{M}$  Et in the presence of caffeine (inset b).

inferred that addition of caffeine reduces the fraction of Et molecules bound to DNA from 98 to 74% and the released Et mostly gets bound to caffeine as indicated by the 7.0 ns component (22%) and a small fraction (2%) goes into the buffer. The uncertainty range in the lifetime measurements is  $\pm 5\%$ . Our experimental result strongly upholds the deintercalative activity of caffeine reported by Johnson et al.<sup>8</sup> However, our work finds inimitability in characterizing the 7.0 ns component (characteristic lifetime of Et complexed with caffeine) which further clarifies the process. By measuring the relative weightage of the 21 ns component, which is a signature of the total population of Et bound to DNA, and knowing the total concentration of Et and DNA molecules in the solution, we calculate the binding constant ( $K$ ) of the ligand Et with DNA using the following equation<sup>16</sup>

$$K = \frac{[\text{Et-DNA}]}{([\text{Et}] - [\text{Et-DNA}])([\text{DNA}] - [\text{Et-DNA}])} \quad (4)$$

where  $[\text{Et-DNA}]$ ,  $([\text{Et}] - [\text{Et-DNA}])$ , and  $([\text{DNA}] - [\text{Et-DNA}])$  represent the concentration of the Et–DNA complex and free Et and free DNA in the solution, respectively. The binding constant of Et with DNA is calculated to be  $(15.4 \pm 1.1) \times 10^4 \text{ M}^{-1}$ , which is comparable to the binding constant value of Et with genomic DNAs reported earlier.<sup>16,18</sup> In the presence of caffeine the binding constant value reduces to  $(7.6 \pm 0.5) \times 10^3 \text{ M}^{-1}$  as part of the free Et is sequestered by free caffeine leading in this way to a shift of the equilibrium between Et not bound to DNA and Et bound to DNA, whereas the value for caffeine solution is calculated to be  $54.6 \pm 3.8 \text{ M}^{-1}$ , which is also in close approximation of that reported earlier.<sup>18</sup> We calculate the free energy change associated with the complex



**Table 2. Variation of Fluorescence Transients of DNA Bound Ethidium ([DNA]:[Et] = 8:1) with Temperature (Error,  $\pm 5\%$ )<sup>a</sup>**

temperature (°C)	$\tau_1$ (ns)	A <sub>1</sub> (%)	$\tau_2$ (ns)	A <sub>2</sub> (%)
18	22	97	2.1	3
30	22	95	2.1	5
42	21	95	1.6	5
52	20	91	1.5	9
61	19	79	1.4	21
71	18	55	1.4	45

<sup>a</sup>  $\tau$  represents the time constant, and A represents the relative contribution of the component.

**Table 3. Variation of Fluorescence Transients of DNA-Bound Ethidium ([DNA]:[Et] = 8:1) with Temperature in the Presence of 100 mM Caffeine (Error,  $\pm 5\%$ )<sup>a</sup>**

temperature (°C)	$\tau_1$ (ns)	A <sub>1</sub> (%)	$\tau_2$ (ns)	A <sub>2</sub> (%)	$\tau_3$ (ns)	A <sub>3</sub> (%)
18	22	60	7	35	1.7	5
30	22	57	6.4	38	1.5	5
42	22	46	6.05	48	1.35	6
52	22	35	5.67	58	1.36	7
61	22	21	5.5	65	1.69	14
71	22	10	4.68	76	1.5	14

<sup>a</sup>  $\tau$  represents the time constant, and A represents the relative contribution of the component.

formation using the equation

$$\Delta G^\circ = -RT \ln K \quad (5)$$

and it is found that the difference in the free energy between the intercalated Et ( $-29.6 \pm 0.2 \text{ kJ mol}^{-1}$ ) and Et–DNA–caffeine complex ( $-22.15 \pm 0.15 \text{ kJ mol}^{-1}$ ) is more than compensated for by the binding of Et with caffeine ( $-9.9 \pm 0.2 \text{ kJ mol}^{-1}$ ), which makes the deintercalation process of caffeine energetically favorable.

To determine the thermal stability of the caffeine–Et complex, we perform temperature-dependent time-resolved experiments (Figure 2). We first monitor the release of DNA intercalated Et into the buffer with rise in temperature as depicted in Figure 2a. As the temperature rises DNA melts with subsequent release of the intercalated Et into buffer, as evidenced through the rise in amplitude of the faster lifetime component of  $\sim 2$  ns from 3 to 45% as temperature rises from 18 to 71 °C (Table 2). Upon addition of 100 mM caffeine in the DNA–Et system we monitor the temperature-dependent change in the lifetime of the Et, as shown in Figure 2b and Table 3. While, in the absence of caffeine, Et is released from the intercalated to the free state in buffer with the progress in DNA melting, in the presence of caffeine most of the released Et, from the DNA intercalated state, heteroassociates with the available caffeine in the solution, as has been observed from the rise in the amplitude of the lifetime component of Et characteristic of its heteroassociation with caffeine, with a minor rise in the amplitude of the faster component of  $\sim 2$  ns from 5 to 14% over the same range of temperature. Since most of the released Et from the DNA bound state remains in a strong heteroassociation with the caffeine molecules in the solution even at high temperature at around 71 °C, it can be concluded that the complex that forms between caffeine and Et is thermally stable and caffeine can perform its deintercalative activity even at high temperature. For further

**Table 4. Variation of Fluorescence Transients of Ethidium (12.5  $\mu\text{M}$ ) with Temperature in the Presence of 100 mM Caffeine (Error,  $\pm 5\%$ )<sup>a</sup>**

temperature (°C)	$\tau_1$ (ns)	A <sub>1</sub> (%)	$\tau_2$ (ns)	A <sub>2</sub> (%)
18	7.15	88	2	12
30	6.6	89	1.8	11
41	6.06	89	1.7	11
50	5.56	88	1.7	12
61	5	88	1.6	12
71	4.4	88	1.5	12

<sup>a</sup>  $\tau$  represents the time constant, and A represents the relative contribution of the component.

confirmation of the thermal stability of the caffeine–Et complex we monitor the temperature-dependent fluorescence transient of Et in the presence of a high caffeine concentration (Figure 2b, inset and Table 4). As depicted in Figure 2b (inset) and Table 4, the amplitude of the faster component of  $\sim 2$  ns, which represents the fraction of free Et present in the buffer, does not change with a rise in temperature, which reconfirms the high stability of the caffeine–Et complex both within and beyond the physiological temperatures.

The mode of interaction of caffeine with the DNA intercalator Et was studied using NMR spectroscopy. All observable protons in Et and caffeine were assigned and were followed in a NMR experiment where 1.78 mM Et was titrated with caffeine. The changes in the chemical shift of Et protons ( $\Delta\delta_{\text{obs}} = \delta_{\text{with caffeine}} - \delta_{\text{no caffeine}}$ ) are shown in Figure 3a. All proton signals (the Et CH<sub>2</sub> signal overlapped with H<sub>2</sub>O signal and was not monitored) exhibited a hyperbolic change indicating Et–caffeine binding. Changes in  $\Delta\delta_{\text{obs}}$  of individual <sup>1</sup>H chemical resonances in Et, upon titration with caffeine, were fitted with eq 6<sup>19</sup> for obtaining the association constant  $K_a$  ( $[C]_T$  and  $[E]_T$  are the total concentrations of caffeine and Et, respectively, and  $\Delta\delta^{\text{max}}$  is the value of  $\Delta\delta_{\text{obs}}$  for a large excess of  $[C]_T$ ).

$$\Delta\delta_{\text{obs}} = \frac{\Delta\delta^{\text{max}}}{2K_a[E]_T} [1 + K_a([C]_T + [E]_T) - \sqrt{\{1 + K_a([C]_T + [E]_T)\}^2 - 4K_a^2[C]_T[E]_T}] \quad (6)$$

As can be observed from Figure 3a,  $K_a$  values were different depending on which protons one monitored;  $K_a \sim 12 \text{ M}^{-1}$  (positions 4 and 7),  $\sim 20 \text{ M}^{-1}$  (positions 2 and 9),  $\sim 30 \text{ M}^{-1}$  (positions 1 and 10), and  $\sim 65\text{--}73 \text{ M}^{-1}$  (for CH<sub>3</sub> and the ortho proton of the Et benzene ring), the latter matching best with the estimate from time-resolved data (this work) and a previous report based on UV–vis absorption spectroscopy.<sup>13</sup> The range of  $K_a$  values obtained from NMR spectroscopy reflects structural heterogeneity of the Et–caffeine complex, undetected by optical spectroscopy. This is consistent with the broad distribution observed from DLS studies around a dominant conformation (discussed later; see Figure 5a). The nature of the dominant conformation can be understood by a careful analysis of ring current shifts observed in Et as a function of added caffeine. During Et–caffeine interaction, the degree of change in  $\Delta\delta_{\text{obs}}$  (and  $K_a$ ) varied in a symmetric fashion (equivalence of 1–10, 2–9, and 4–7 positions) across the Et molecule. In addition, while positions 1, 10, 2, 9, 4, and 7 exhibited a negative  $\Delta\delta_{\text{obs}}$ , the benzyl ortho position and the CH<sub>3</sub> protons of Et showed a positive  $\Delta\delta_{\text{obs}}$ . The major cause of chemical shift change in Et,

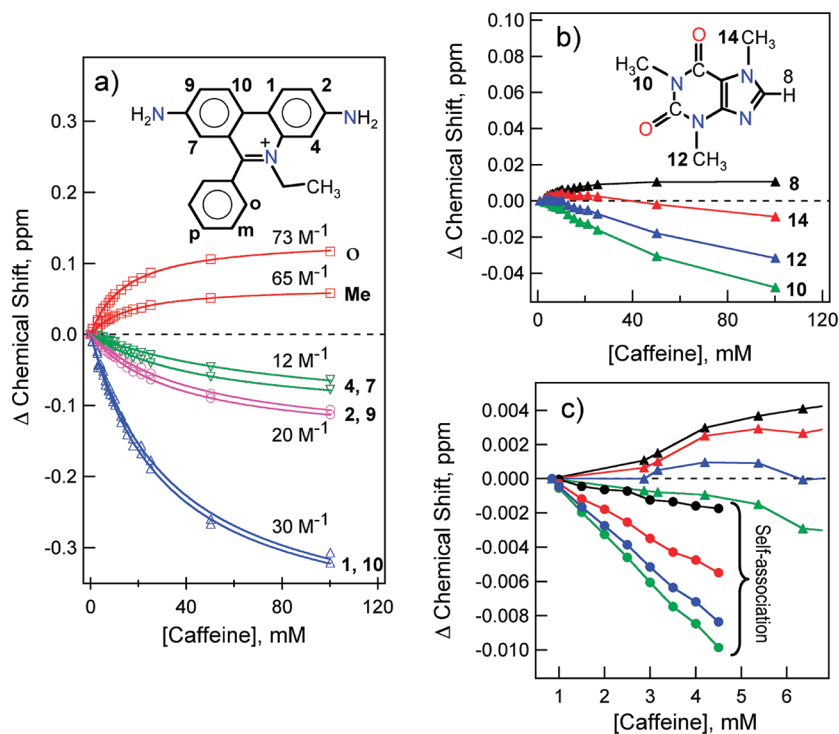


**Figure 3.**  $^1\text{H}$  chemical shift changes observed during titration of Et (1.78 mM) by caffeine (pH 7.0, 25 °C): (a) Et; (b) caffeine.  $^1\text{H}$  resonance signals are annotated with atom numbers, corresponding to the molecules shown in the panels. The continuous lines in panel a correspond to the best fits with eq 6 with the corresponding  $K_a$  values reported above each fit. Panel c shows changes in caffeine  $^1\text{H}$  chemical shifts for early data points (0–6 M) of panel b along with  $^1\text{H}$  chemical shift changes in caffeine due to self-association (concentration dependence) in the same concentration range. Atom numbering (colors) in panel c is identical to that in panel b.

due to interaction with caffeine, must originate from ring current shifts, producing positive and negative  $\Delta\delta_{\text{obs}}$ . Placement of an Et proton directly above the caffeine ring (stacking) will produce a negative  $\Delta\delta_{\text{obs}}$  while positioning of Et protons in the plane of the caffeine ring will produce a positive  $\Delta\delta_{\text{obs}}$ .

On the basis of the NMR data (symmetry of  $K_a$  and  $|\Delta\delta_{\text{obs}}|$ ) and the assumption that the sign of  $\Delta\delta_{\text{obs}}$  originates from the ring current effect, a model for a 1:1 complex of caffeine:Et was constructed as shown in Figure 4b. Caffeine and Et molecules are stacked in the 1:1 model where the  $\text{CH}_3$  and the *o*-benzyl protons of Et (shown as magenta spheres in Figure 4b) protrude toward the plane of the caffeine ring, giving rise to the observed positive  $\Delta\delta_{\text{obs}}$ . The stacked caffeine can flip, effectively making its effect on the Et symmetric. The flipping is consistent with a model of caffeine dimer where two forms of caffeine dimers (flipped and unflipped stacking, Figure 4a) have been observed.<sup>20</sup> Our model suggests that two protons in caffeine, positions 8 and 14 (shown as magenta spheres in Figure 4b), should also exhibit a positive  $\Delta\delta_{\text{obs}}$  (ring current effect from Et). To validate this, caffeine chemical shifts were monitored in the Et titration experiment of Figure 3a and are shown in Figure 3b. Indeed positions 8 and 14 of caffeine showed a positive  $\Delta\delta_{\text{obs}}$  as expected from the model. This becomes more clear in Figure 3c where the early data points are shown (up to 4:1 caffeine:Et ratio) along with caffeine self-association data (all resonances in the self-association show negative  $\Delta\delta_{\text{obs}}$ ).

To determine the size of the complex formed between caffeine and Et, we performed DLS experiments and the results are shown in Figure 5a. The DLS data, with broad peaks for caffeine, in the presence and in absence of Et, indicate a distribution of populations

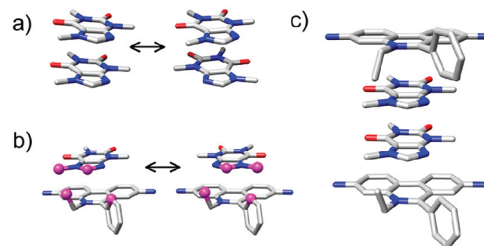


**Figure 4.** (a) Interconverting caffeine dimers (stacked on each other). (b) Model for interconverting 1:1 complex of caffeine and Et, compatible with NMR titration data.  $^1\text{H}$  resonances that exhibited downfield shift upon complex formation (positions 8 and 14 in caffeine, and ortho and Me in Et; Figure 3) are shown as ball and stick model (magenta). (c) Model of 2:2 caffeine:Et complex compatible with caffeine:caffeine stacking (panel a) and caffeine:Et stacking (panel b). The structures were energy minimized to remove steric clashes.

around a dominant structure and consistent with NMR data. The DLS-derived hydrodynamic diameter (corresponding to the peak of the distributions) of 100 mM caffeine is 8.4 Å. This increases to 14.2 Å upon addition of 25  $\mu\text{M}$  Et. Fluorescence anisotropy studies on Et (Figure 5b), in the presence of caffeine, yielded a hydrodynamic diameter of 12.3 Å, slightly lower than the DLS-derived value. To compare with the experimental values, hydrodynamic diameters of caffeine dimer (Figure 4a) and the 2:2 caffeine:Et complex (Figure 4c) were estimated using the program Hydropro.<sup>21</sup> The calculated diameters, 8.9 Å for caffeine dimer, and 13.0 Å for the 2:2 caffeine:Et complex, are compatible with the experimental data. The above analysis shows that the major component of pure caffeine is the dimeric form. In the presence of Et, caffeine:Et complexes with a

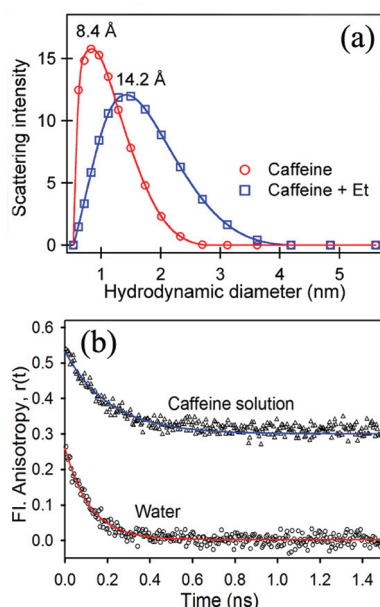


**Figure 5.** (a) Dynamic light scattering of 100 mM caffeine with (blue squares) and without (red circles) 25  $\mu$ M ethidium. (b) Fluorescence anisotropy of Et in water ( $\circ$ ) and in the presence of 100 mM caffeine ( $\Delta$ ). The baseline for anisotropy of Et in caffeine solution has been shifted vertically by 0.3 for better clarity.

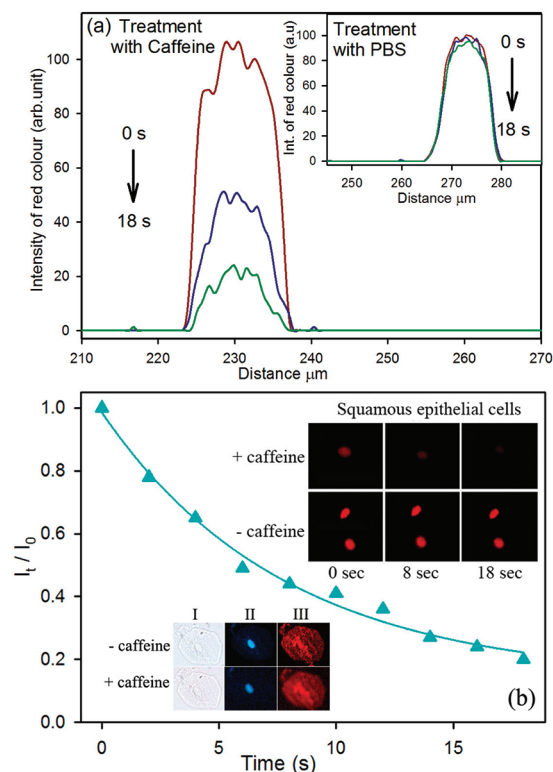


**Figure 7.** (a) Reduction in intensity of red color with time when squamous epithelial cells are treated with caffeine and PBS as control (inset). (b) Rate of leaching out of Et from nucleus of squamous epithelial cells when treated with caffeine.  $I_t$  and  $I_0$  represents the emission intensity of Et at time  $t$  and initially, respectively. Upper right inset shows the fluorescence micrographs of Et stained same cells initially, after 8 s and after 18 s upon treatment with caffeine along with the control sets. Lower left inset shows the morphology of the same cell line before and after 5 min upon caffeine treatment under bright-field (I) and fluorescence micrographs of the same stained with DAPI (II) and merocyanine 540 (III).

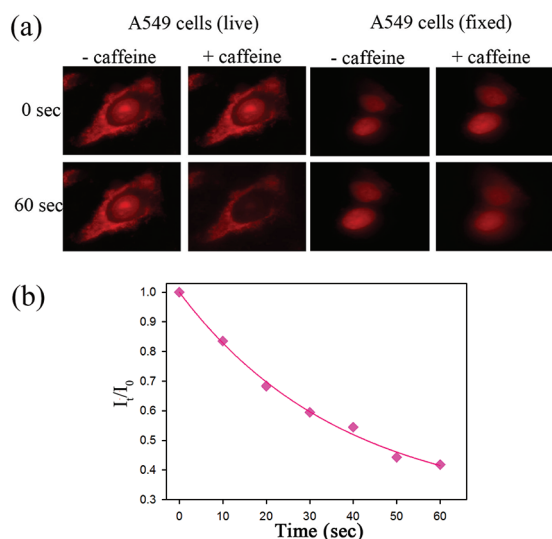


**Figure 6.** (a) Fluorescence micrographs of both live and fixed Et stained A549 cells initially and after 60 s upon treatment with caffeine (+ caffeine) along with the control sets (– caffeine) treated with PBS without caffeine. (b) Rate of leaching out of Et from the nucleus of live A549 lung carcinoma cells when treated with caffeine.  $I_t$  and  $I_0$  represents the emission intensity of Et at time  $t$  and initially, respectively.

2:2 (or higher) stoichiometry dominate. Incidentally, no peaks were obtained at higher hydrodynamic radii, indicating the absence of any higher order aggregation.

Our spectroscopic results reflecting the efficacy of caffeine in the extraction of Et upon forming a caffeine–Et complex with it provoke us to get a microscopic view of such activity of caffeine molecules. To study in biological milieu, we have used some animal cell lines. Figure 6a shows the fluorescence micrographs

of both live and fixed A549 cells stained with Et and subsequently treated with caffeine (“+ caffeine”), and for control experiment identical sets of stained cells were treated with PBS without caffeine (“– caffeine”). Comparing the fluorescence micrographs of both live and fixed + caffeine and – caffeine cells after 60 s of treatment, we observe there is a significant drop in the emission intensity of Et from the nucleus of the live A549 cells treated with caffeine. The drop in emission intensity of Et can be explained in terms of the efficiency of caffeine molecules in removal of Et from the nucleus of those live cells. As evident from the fluorescence micrographs of Figure 6a, the efficacy of caffeine in the extraction of Et from the nucleus of fixed cells is less compared to the live ones. To get insight into the kinetics of the extraction process, we plot  $I_t/I_0$  against time (Figure 6b), where  $I_t$  represents the emission intensity of Et in the nucleus at time  $t$  and  $I_0$  represents the same initially just after the addition of caffeine to the live A549 stained cells. We fit the curve with single-exponential decay and find the extraction of Et from the cell nucleus of live A549 cells by caffeine with a characteristic time constant of 38 s.

After monitoring the effect of caffeine on A549 cells, we proceed with squamous epithelial cells taken from the human mouth. Et, being a potential intercalator of DNA,<sup>22</sup> binds only in the nucleus of the cell, and the red emission observed in the



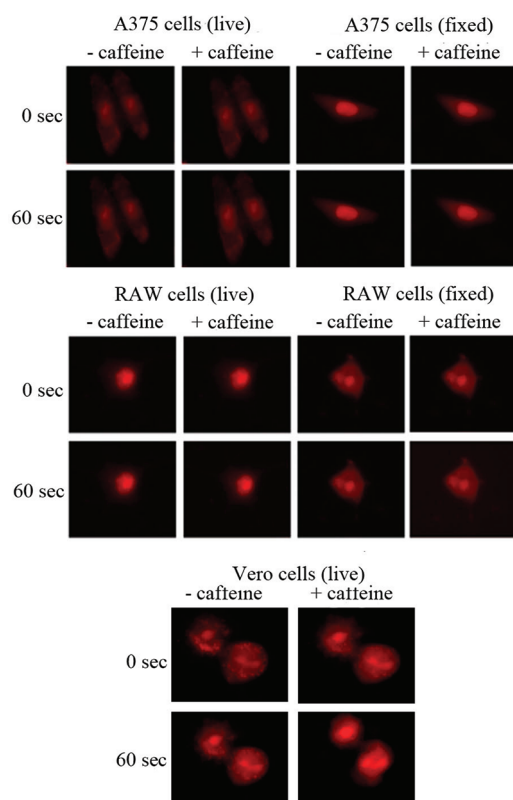


**Figure 8.** Fluorescence micrographs of Et stained A375 and RAW cells (both live and fixed) along with Vero (live) cells treated with caffeine (+ caffeine) and images taken at 0 and 60 s interval. The control sets (– caffeine) are treated with PBS without caffeine.

micrographs (Figure 7b, upper right inset) are due to the Et that emits in the red region ( $\sim 600$  nm).<sup>16</sup> As can be observed from the figure, when the stained cells are treated with caffeine (+ caffeine), Et is released from the nucleus at a very fast rate. The intensity of red color of the cells is blurred with time, which indicates release of Et from the nucleus. In the control experiment (– caffeine) cells retain almost the entire amount of Et in their nucleus. To highlight the deintercalative property of caffeine in a more quantitative manner, the intensity of the red color of Et from the cell nucleus, which is proportional to the amount of Et present, has been plotted at regular time interval for both systems (– caffeine and + caffeine), where the  $X$ -coordinate represents the distance in the horizontal plane where the cell lies (Figure 7a). As evident from the figure the intensity of red color is considerably high at the position that corresponds to the cell nucleus and it falls rapidly after 8 s (blue line) upon treatment with caffeine solution, whereas a negligible change is produced in the control set (– caffeine) within the same time scale (Figure 7a, inset). After 18 s, + caffeine cells show a negligible amount of Et left in their nucleus (green line) while no significant change has been observed in – caffeine cells. As a control study to rule out the possibility of cell disruption upon treatment with caffeine, we have taken the cell images (Figure 7b, lower left inset) under bright field before and after treating them with caffeine and found no change even after 5 min. In addition, we stained the cell nuclei with a fluorescent dye, DAPI and found that cell nuclei remain intact over the same time span upon treatment with caffeine. Furthermore, we checked the membrane integrity of the cells by staining them with another fluorescent dye, merocyanine 540, and found that the cell membranes

remain unperturbed upon treatment with caffeine. The plot of  $I_t/I_0$  against time (Figure 7b) gives the characteristic time constant for extraction of Et from these cells by caffeine as 8 s. However, no significant result has been observed in the removal of Et from A375, RAW, and Vero cell lines by caffeine (Figure 8).

## CONCLUSION

Our steady-state and time-resolved fluorescence studies with synthetic DNA emphasize the interceptive role of well-consumed caffeine molecules, forming heterocomplexes with Et. Temperature-dependent picosecond-resolved fluorescence experiments highlight the thermal stability of such complexes within and beyond the physiological temperature. Results from NMR and DLS studies were used to construct a model of caffeine–Et dimer representing the dominant structure of Et–caffeine complex in solution. Our cellular studies reveal the precise nature of the xanthine alkaloid in the exclusion of mutagenic Et from the cell nucleus. The specific molecular interaction of caffeine with Et molecule underlying the “interceptor” action of caffeine can be considered as one of the potential mechanisms of Et release in our present study. For the physiological activity of the drugs in the presence of caffeine another mechanism of action called “protector” can also occur, in which there is a competition between caffeine and Et for the binding sites on DNA. It is likely that both mechanisms can act simultaneously and therefore must be taken into consideration when analyzing a three-component equilibrium of the Et, caffeine, and DNA. We believe that our studies may find relevance in the therapeutic use of caffeine as the noninvasive antimutagenic agent particularly for the prevention of oral cancers/squamous cell carcinomas which arises due to the activation of oncogenes as a result of DNA mutation.

## AUTHOR INFORMATION

### Corresponding Author

\*E-mail: skpal@bose.res.in. Fax: 91 33 2335 3477.

## ACKNOWLEDGMENT

S.B. thanks UGC, and P.K.V. thanks CSIR for a Research Fellowship. We thank DST for a financial grant (SR/SO/BB-15/2007). We thank Saumya Dasgupta and Barun Majumder for their assistance in estimation of the hydrodynamic diameter and NMR experiments, respectively. D.B. is a SRF of RFSMS under UPE (UGC) awarded to the University of Calcutta, and A.S. is supported by grants from DBT (BT/PR 11415/BRB/10/656/2008) and DST (SR/SO/HS-51/2008) of the Government of India.

## REFERENCES

- (1) Selby, C. P.; Sancar, A. *Proc. Natl. Acad. Sci. U. S. A.* **1990**, *87*, 3522.
- (2) Traganos, F.; Kapuscinski, J.; Darzynkiewicz, Z. *Cancer Res.* **1991**, *51*, 3682.
- (3) Larsen, R. W.; Jasuja, R.; Hetzler, R. K.; Muraoka, P. T.; Andrada, V. G.; Jameson, D. M. *Biophys. J.* **1996**, *70*, 443.
- (4) Ganapathi, R.; Grabowski, D.; Schmidt, H.; Yen, A.; Iliakis, G. *Cancer Res.* **1986**, *46*, 5553.
- (5) Kimura, H.; Aoyama, T. *J. Pharmacobio-Dyn.* **1989**, *12*, 589.
- (6) Traganos, F.; Kaminska-Eddy, B.; Darzynkiewicz, Z. *Cell Proliferation* **1991**, *24*, 305.
- (7) Mahler, H. R.; Perlman, P. S. *Arch. Biochem. Biophys.* **1972**, *148*, 115.

- (8) Johnson, I. M.; Kumar, S. G. B.; Malathi, R. *J. Biomol. Struct. Dyn.* **2003**, *20*, 677.
- (9) Mezey, E.; Chandross, K. J.; Harta, G.; Maki, R. A.; McKercher, S. R. *Science* **2000**, *290*, 1779.
- (10) Easton, T. G.; Valinsky, J. E.; Reich, E. *Cell* **1978**, *13*, 475.
- (11) Siddhanta, A.; Backer, J. M.; Shields, D. *J. Biol. Chem.* **2000**, *275*, 12023.
- (12) Connor, D. V. O.; Philips, D. *Time Correlated Single Photon Counting*; Academic Press: London, 1984.
- (13) Philips, L. A.; Webb, S. P.; Clark, J. H. *J. Chem. Phys.* **1985**, *83*, 5810.
- (14) Kalman, B.; Clarke, N.; Johansson, L. B. A. *J. Phys. Chem.* **1989**, *93*, 4608.
- (15) Sitkowski, J.; Stefaniak, L.; Nicol, L.; Martin, M. L.; Martin, G. J.; Webb, G. A. *Spectrochim. Acta, Part A* **1995**, *51*, 839.
- (16) Sarkar, R.; Pal, S. K. *Biopolymers* **2006**, *83*, 675.
- (17) Davies, D. B.; Veselkov, D. A.; Djimant, L. N.; Veselkov, A. N. *Eur. Biophys. J.* **2001**, *30*, 354.
- (18) Baranovsky, S. F.; Bolotin, P. A.; Evstigneev, M. P.; Chernyshev, D. N. *J. Appl. Spectrosc.* **2009**, *76*, 132.
- (19) Hirose, K. *J. Incl. Phenom. Macrocyclic Chem.* **2001**, *39*, 193.
- (20) Falk, M.; Chew, W.; Walter, J., A.; Kwiatkowski, W.; Barclay, K. D.; Klassen, G. A. *Can. J. Chem.* **1998**, *76*, 48.
- (21) Ortega, A.; Amoros, D.; García de la Torre, J. *Biophys. J.* **2011**, *101*, 892.
- (22) Lai, J. S.; Herr, W. *Proc. Natl. Acad. Sci. U. S. A.* **1992**, *89*, 6958.